



Differential hepatic mitochondrial function and gluconeogenic gene expression in 2 Holstein strains in a pasture-based system

Mercedes García-Roche,^{1,2*} Daniel Talmón,¹ Guillermo Cañibe,¹ Ana Laura Astessiano,¹ Alejandro Mendoza,^{2,3} Celia Quijano,² Adriana Cassina,² and Mariana Carriquiry¹

¹Departamento de Producción Animal y Pasturas, Facultad de Agronomía, Universidad de la República, 12900, Montevideo, Uruguay

²Centro de Investigaciones Biomédicas (CEINBIO) and Departamento de Bioquímica, Facultad de Medicina, Universidad de la República, 11900, Montevideo, Uruguay

³Programa Nacional de Producción de Leche, Instituto Nacional de Investigación Agropecuaria, 39173, Semillero, Uruguay

ABSTRACT

The objective of this study was to assess hepatic ATP synthesis in Holstein cows of North American and New Zealand origins and the gluconeogenic pathway, one of the pathways with the highest ATP demands in the ruminant liver. Autumn-calving Holstein cows of New Zealand and North American origins were managed in a pasture-based system with supplementation of concentrate that represented approximately 33% of the predicted dry matter intake during 2017, 2018, and 2019, and hepatic biopsies were taken during mid-lactation at 174 ± 23 days in milk. Cows of both strains produced similar levels of solids-corrected milk, and no differences in body condition score were found. Plasma glucose concentrations were higher for cows of New Zealand versus North American origin. Hepatic mitochondrial function evaluated measuring oxygen consumption rates showed that mitochondrial parameters related to ATP synthesis and maximum respiratory rate were increased for cows of New Zealand compared with North American origin. However, hepatic gene expression of pyruvate carboxylase, phosphoenolpyruvate carboxykinase, and pyruvate dehydrogenase kinase was increased in North American compared with New Zealand cows. These results altogether suggest an increased activity of the tricarboxylic cycle in New Zealand cows, leading to increased ATP synthesis, whereas North American cows pull tricarboxylic cycle intermediates toward gluconeogenesis. The fact that this occurs during mid-lactation could account for the increased persistency of North American cows, especially in a pasture-based system. In addition, we observed an augmented mitochondrial density in New Zealand cows, which could be related to feed efficiency

mechanisms. In sum, our results contribute to the elucidation of hepatic molecular mechanisms in dairy cows in production systems with higher inclusion of pastures. **Key words:** intermediary metabolism, gluconeogenesis, dairy cows, grazing, Holstein-Friesian

INTRODUCTION

In addition to the benefits in product quality (O'Callaghan et al., 2016), the inclusion of pastures in dairy cow systems results in lower feeding costs and, in consequence, a system more resilient to the volatility of markets, especially for exporting countries (Fariña and Chilibróste, 2019). Productive performance of pasture-based dairy systems is very much related to grazing management to ensure sufficient DM intake, which is generally reduced compared with confined systems, and appropriate quality of pastures (Chilibróste et al., 2012). Also, intrinsic to pasture-based systems is the greater energy expenditure due to walking and grazing activities (Jasinsky et al., 2019). Previous authors have shown that when nutrient concentration is insufficient, cows may show a poor metabolic status, as negative energy balance markers such as plasma nonesterified fatty acids and BHB and liver triglyceride concentrations are exacerbated (Meikle et al., 2013; García-Roche et al., 2021). Furthermore, hepatic energy metabolism has also been reported to be compromised in cows managed under a pasture-based system, as mitochondrial function is impaired during early lactation (García-Roche et al., 2019).

The genetic selection process of North American (NAH) and New Zealand (NZH) Holstein strains determined differences in their productive and reproductive performance in a pasture-based system. Although NAH produce more milk than NZH cows, the latter produce greater percentages of milk solids (Lucy et al., 2009; White et al., 2012). In addition, NAH cows are unable to maintain an acceptable body condition and

Received September 30, 2021.

Accepted March 17, 2022.

*Corresponding author: mercedesg@fagro.edu.uy

weight during lactation and fail to maintain a 365-d calving interval, yielding poorer fertility and survival performance compared with NZH cows in grazing systems (Kolver et al., 2000; Harris and Kolver, 2001). Also, NZH cows have a lower energy requirement for maintenance than NAH cows (Talmón et al., 2020). Differences among strains have been associated with reduced uncoupling of the somatotrophic axis and insulin resistance during the transition period in NZH compared with NAH cows (Chagas et al., 2006; Lucy et al., 2009). Additionally, previous research indicates differences between Holstein strains in hepatic energy metabolism; cows of NZH origin presented increased expression of pyruvate carboxylase (*PC*) mRNA, which could translate into a more active tricarboxylic acid (*TCA*) cycle (White et al., 2012). Altogether, these results could lead to higher intermediary metabolism activity for NZH cows and, thus, increased availability of oxidative phosphorylation precursors for NZH cows compared with NAH cows in a grazing system. Thus, we hypothesized that mitochondrial ATP synthesis would be increased in NZH cows relative to NAH cows. Therefore, in pasture-based systems, NZH cows would be better prepared to face the energy demands imposed by anabolic routes and other activities, as a result of increased ATP availability. Hence, our objective was to study the potential for hepatic ATP synthesis in diverging Holstein strains in a pasture-based system and its interplay with a highly energy-demanding pathway: gluconeogenesis.

MATERIALS AND METHODS

The experiment was conducted at the Experimental Station of the Instituto Nacional de Investigación Agropecuaria (Colonia, Uruguay) during the spring of 2017, 2018, and 2019. Animal use and procedures were approved by the Animal Experimentation Committee of the Instituto Nacional de Investigación Agropecuaria, Uruguay (file number: INIA2017.2).

The experiment formed part of a larger study designed to evaluate the effect of cow genotype (NZH vs. NAH strains) in different feeding strategies on individual animal and whole-farm biophysical performance. More detailed descriptions of Holstein strains, animal and grazing management, as well as milk production, BW, and BCS from June 2017 through May 2019 were previously reported (Stirling et al., 2021).

Experimental Design

Autumn-calving Holstein cows of NZH (512 ± 19 kg BW and 3.07 ± 0.12 BCS at calving; $n = 12$) and NAH strains (563 ± 29 kg BW, 3.10 ± 0.1 BCS at calving; n

$= 18$) were used to evaluate 10 cows of each genotype for 3 yr. In the NZH group, 7 cows were evaluated for 3 yr, 4 for 2 yr, and 1 additional cow only in yr 3. In the NAH group, 3 cows were evaluated for 3 yr, 4 for 2 yr, and 11 only for 1 yr.

Both NZH and NAH strains had at least 75% of each cow's ancestors (2 generations: father and maternal grandfather) from New Zealand or from the United States or Canada, respectively (Stirling et al., 2021). In the present study, the NZH and NAH strains presented progeny of 7 sires in each group. The economic and productive selection index was 126 ± 11 and 105 ± 14 on average for NZH and NAH cows, respectively. Expected progeny differences were -187.6 ± 164 kg, $+0.170 \pm 0.111\%$, and $+0.157 \pm 0.145\%$ for milk yield, milk fat, and milk protein content for NZH cows, and $+44.9 \pm 174$ kg, $+0.086 \pm 0.064\%$, and $+0.004 \pm 0.068\%$ for milk yield, milk fat, and milk protein content for NAH cows (Mejoramiento y Control Lechero Uruguayo; <https://www.mu.org.uy>).

Cows were paired in each strain group according to their calving date (May 4, 2017, ± 17 d; May 5, 2018, ± 23 d; May 2, 2019, ± 37 d) and lactation number (2.12 ± 0.8 lactations). Cows were managed in a mixed grazing system: during mid-lactation, cows grazed on daily strips of orchardgrass (*Dactylis glomerata*) and alfalfa (*Medicago sativa*) or fescue (*Festuca arundinacea*) in a rotational-grazing manner during 2 grazing sessions (a.m. and p.m. session: from 0500 to 1400 h and from 1500 to 0400 h, respectively). Average herbage mass was $1,713 \pm 423$ kg of DM/ha; 5 cm above ground level. Each strain group grazed on separate paddocks to ensure similar pasture allowance relative to their BW (11.2 ± 0.9 kg of DM/cow per day for NZH and 14.9 ± 1.5 kg of DM/cow per day for NAH, 5 cm above ground level, 3-yr average). Fresh water was offered in each paddock. Predicted DM intake was estimated according to the National Research Council model for dairy cattle (NRC, 2001). Hence, when forage allowance was considered restrictive, cows were supplemented with conserved forage (corn silage and pasture haylage mix in a 67:33 ratio, 3-yr average) to achieve predicted DM intake. Pasture forage allowance and haylage supplementation were adjusted weekly based on weekly pasture growth. Details of the grazing management were presented previously (Talmón et al., 2020; Stirling et al., 2021), and chemical composition and metabolizable energy concentration of feedstuffs are presented in Table 1. Briefly, pasture was offered in daily strips, which cows of each genotype grazed separately to keep similar herbage allowance relative to their BW and to ensure breeds behaved independently and avoid dominance. As cows grazed pastures in a rotational-grazing manner, they returned to defined

grazing areas once most of the grass tillers had between 2.5 and 3 leaves.

Cows were milked twice a day and supplemented with concentrate (33% of predicted daily DM intake, 6.8 ± 0.4 kg of DM/d for NZH, and 7.5 ± 0.9 kg of DM/d for NAH, 3-yr average). Milk yield was recorded daily, and milk samples were collected every 14 d. Solids-corrected milk (SCM) was calculated as SCM (kg) = 12.3 (F) + 6.56 (SNF) – 0.0752 (M), where F, SNF, and M are expressed as kilograms of fat, solids-not-fat, and milk, respectively (Tyrrell and Reid, 1965). As this work is part of a larger study, cow BCS (score 1 to 5; Edmonson et al., 1989) was determined every 14 d by one evaluator (Stirling et al., 2021).

Plasma Collection and Liver Biopsies

Plasma samples and liver biopsies were collected in the spring during the months of October and November of 2017, 2018, and 2019 (at 187 ± 19 , 176 ± 21 , and 158 ± 29 DIM, respectively, in average 174 ± 23 DIM, mid-lactation). In this period, cows were in either the first or the second trimester of gestation (96 ± 38 d of gestation for NZH, and 78 ± 41 d of gestation for NAH). Indeed, this study is part of a larger study, which reported calving to conception days: 96.3 and 108.1 ± 4.9 (SEM), respectively, for NZH and NAH (Stirling et al., 2021).

Plasma samples were collected by venipuncture of the coccygeal vein using 10-mL heparinized Vacutest tubes (Vacutest Kima). Samples were centrifuged at $4,000 \times g$ for 12 min and immediately stored at -20°C until analysis. Biopsies were taken using a 14-gauge biopsy needle (Tru-Core-II Automatic Biopsy Instrument; Angiotech) after local intramuscular administration of 3 mL of 2% lidocaine hydrochloride (Carrquiry et al., 2009) and either cryopreserved for mitochondrial oxygen consumption analyses (García-Roche et al., 2018)

Table 1. Chemical composition and ME concentration (means \pm SD) of feedstuffs offered during the experiment

Item	Pasture ¹	Concentrate ²	Conserved forage ³
DM (%)	23.0 ± 1.7	90.0 ± 1.3	45.1 ± 8.2
CP (% DM)	22.7 ± 3.8	19.6 ± 1.6	12.3 ± 2.8
NDF (% DM)	48.6 ± 3.4	35.7 ± 7.3	42.6 ± 9.5
ADF (% DM)	28.3 ± 4.1	19.1 ± 7.5	27.1 ± 7.3
Ash (% DM)	10.7 ± 0.5	7.9 ± 0.4	9.55 ± 4.3
ME (Mcal/kg DM)	2.48 ± 0.14	2.91 ± 0.03	2.48 ± 0.18

¹*Dactylis glomerata* and *Medicago sativa* or *Festuca arundinacea*.

²Commercial concentrate (Prolacta 18, Prolesa S.A.) composed of corn grain, soybean meal, wheat bran, and vitamin and mineral mix. The SD represents the variation between feedstuff samples collected during the measurement period of the 3 yr of the experiment (2017, 2018, 2019).

³Corn silage and pasture haylage mix.

or immediately frozen in liquid nitrogen. All samples were stored at -80°C until analysis.

Plasma and Hepatic Metabolites

Plasma glucose, urea, BHB, and nonesterified fatty acids (NEFA) were determined spectrophotometrically with commercial kits from Biosystems S.A. for glucose and urea and from Randox Laboratories Ltd. for BHB and NEFA, at $\lambda = 505$ nm, 600 nm, 340 nm, and 560 nm, respectively (Astessiano et al., 2015; García-Roche et al., 2021).

For hepatic free glucose and glycogen quantification, liver homogenates were performed using 500 μL of 2 *N* HCl and glass Dounce homogenizers. Homogenates were subjected to 100°C for an hour, for glycogen digestion to glucose by acid-heat hydrolysis (Bancroft and Fry, 1933). Free liver glucose and digested liver glycogen were determined using a kit from Biosystems S.A., following manufacturer instructions, after neutralizing acid samples with an equal amount of 2 *M* NaOH. Absorbance was measured at $\lambda = 505$ nm.

For liver triglyceride quantification, liver homogenates were obtained according to Armour et al. (2017). Briefly, liver tissue was homogenized in lysis buffer (140 *mM* NaCl, 50 *mM* Tris, and 1% Triton X-100, pH 8) and measured using a kit from Biosystems S.A., following manufacturer instructions at $\lambda = 505$ nm. For all metabolite assays intra- and interassay coefficient of variation (CV) were less than 10%. Liver triglyceride is expressed per unit of tissue protein.

Mitochondrial Oxygen Consumption Rate

Mitochondrial function was studied measuring oxygen consumption rate in a high-resolution Oroboros Oxygraph 2k respirometer (Oroboros Instruments) at 37°C (García-Roche et al., 2018, 2019). Briefly, electrodes were calibrated in modified mitochondrial respiration medium (MIR05; 0.5 *mM* ethylene glycol-bis(β -aminoethyl ether)-*N,N,N',N'*-tetraacetic acid, 3 *mM* $\text{MgCl}_2 \cdot 6\text{H}_2\text{O}$, 60 *mM* 4-morpholinepropanesulfonic acid, 3-(*N*-morpholino)propanesulfonic acid, 20 *mM* taurine, 10 *mM* KH_2PO_4 , 20 *mM* HEPES, 110 *mM* sucrose, 1 g/L BSA, pH 7.1) with a calculated saturated oxygen concentration of 191 μM at 100 kPa barometric pressure at 37°C . Respiratory rates (pmol of O_2 /min per mL) were calculated using DatLab 4 analysis software (Oroboros Instruments). Liver biopsies were weighed (2–10 mg) and added to the chamber, and oxygen consumption measurements were obtained before and after the sequential addition of specific substrates of the respiratory chain, 10 *mM* glutamate and 5 *mM* malate (complex I) or 20 *mM* succinate (complex II),

followed by 4 mM adenosine diphosphate (ADP), 2 μ M oligomycin (ATP synthase inhibitor), 2 to 4 μ M carbonyl cyanide-p-trifluoromethoxyphenylhydrazone (FCCP, an uncoupler of oxidative phosphorylation). Maximum uncoupling was obtained by FCCP titration. It is important to emphasize that the maximum respiratory rate is obtained by maximum uncoupling by means of the titration of FCCP—an uncoupler—to dissipate the proton gradient completely without the regulation of the ADP/ATP ratio (García-Roche et al., 2018). This parameter is indicative of the activity of the electron transport chain complexes or the quantity of mitochondria in the tissue that could be drawn upon in situations of strenuous energy demands or damage (Brand and Nicholls, 2011). Respiration was inhibited with 0.5 μ M rotenone (complex I inhibitor) or 2.5 μ M antimycin A (complex III inhibitor). All respiratory parameters and indices were obtained as described in García-Roche et al. (2018). Briefly, non-mitochondrial oxygen consumption rate measured after the addition of specific inhibitors rotenone or antimycin A and subtracted from all other values before calculating the respiratory parameters. State 4 respiration was determined as the baseline measurement obtained with complex I and II substrates before the addition of ADP, and state 3 was determined after the addition of ADP. Oligomycin-resistant respiration (ATP-independent) was measured after addition of oligomycin, and oligomycin-sensitive respiration (ATP-dependent) was the difference between state 3 and oligomycin-resistant respiration. Finally, the maximum respiratory rate was determined after titration with FCCP. The leaking control ratio was calculated as oligomycin-resistant respiration divided by the maximum respiratory rate, as described previously by Gnaiger (2009) and Koliaki et al. (2015).

RNA Extraction and Quantitative PCR Analysis

Total RNA extraction from liver tissue and cDNA synthesis by reverse transcription was performed (Carriquiry et al., 2009) using the Trizol reagent, followed by lithium chloride precipitation and DNase treatment using an Ambion DNA-Free DNA Removal Kit (Thermo Fisher Scientific). Concentration of RNA was determined by measuring absorbance at $\lambda = 260$ nm (NanoDrop ND-1000 Spectrophotometer; Nanodrop Technologies), and purity and integrity of RNA isolates were assessed from 260/280 and 260/230 absorbance ratios (greater than 1.9 and 1.8, respectively). Samples of RNA were stored at -80°C . A SuperScript III Reverse Transcriptase Kit (Invitrogen from Thermo Fisher Scientific) was used to perform retrotranscription along with random hexamers and 1 μ g of total RNA as a

template. The cDNA was stored at -20°C until its use in the real-time PCR. Primers (Supplemental Table S1, <https://data.mendeley.com/datasets/gx5yh5t2bp/1>) to specifically amplify cDNA of target genes: β -actin (*ACTB*), glucose-6-phosphatase (*G6PC*), hypoxanthine phosphoribosyl transferase (*HPRT1*), methylmalonyl-CoA mutase (*MMUT*), succinate dehydrogenase complex, subunit A, flavoprotein (*SDHA*), pyruvate carboxylase (*PC*), phosphoenolpyruvate carboxykinase (*PCK1*), pyruvate dehydrogenase E1 subunit α 1 (*PDHA1*), pyruvate dehydrogenase kinase (*PDK4*), peroxisome proliferator-activated receptor gamma co-activator 1- α (*PPARGC1A*), peroxisome proliferator-activated receptor α (*PPARA*), sirtuin 1 (*SIRT1*), NADH:ubiquinoneoxidoreductase core subunit V1 (*NDUFV1*, nuclear gene), and mitochondrially encoded cytochrome c oxidase I (*mt-CO1*, mitochondrial gene) were obtained from literature, or specifically designed using the Primer3 website (<http://www.bioinformatics.nl/cgi-bin/primer3plus/primer3plus.cgi>) and bovine nucleotide sequences available from NCBI (<http://www.ncbi.nlm.nih.gov/>).

Real-time PCR reactions were carried out in a total volume of 15 μ L using Maxima SYBR Green/ROX qPCR Master Mix 2X (Thermo Fisher Scientific), using the following standard amplification conditions: 10 min at 95°C and 40 cycles of 15 s at 95°C , 30 s at 60°C , and 30s at 72°C in a 48-well StepOne Real-Time PCR System (Applied Biosystems from Thermo Fisher Scientific). Melting curves were run on all samples to detect primer dimers, contamination, or presence of other amplicons. Each plate was designed including a pool of total RNA from bovine liver samples analyzed in triplicate to be used as the basis for the comparative expression results (exogenous control) and duplicate wells of non-template control (water). Gene expression was determined by relative quantification with respect to the exogenous control (Pfaffl, 2004) and normalized to the geometric mean expression of the endogenous control genes (*ACTB* and *HPRT*). Expression stability of 2 selected housekeeping genes was evaluated using the MS-Excel add-in Normfinder (MDL); values obtained with Normfinder were 0.004 for *ACTB* and 0.003 for *HPRT*. Amplification efficiencies or target and endogenous control genes were estimated by linear regression of a cDNA dilution curve (Supplemental Table S1, <https://data.mendeley.com/datasets/gx5yh5t2bp/1>). Intra- and interassay CV values were less than 1.4 and 2.6% ($n = 5$ dilutions, from 100 to 6.25 ng/well), respectively.

Determination of the ratio of mitochondrial DNA (**mtDNA**) to nuclear DNA (**nDNA**; mtDNA:nDNA) was performed according to Casal et al. (2018). Briefly, real-time PCR reactions prepared in separate tubes to

detect mitochondrial encoded cytochrome c oxidase I (*mt-CO1*, mitochondrial gene) and NADH:ubiquinone oxidoreductase core subunit V1 (*NDUFV1*, nuclear gene), respectively, and real-time PCR reactions were conducted as aforementioned. To calculate the mtDNA:nDNA ratio, the difference between cycle numbers was calculated ($C_{tn} - C_{tmt}$) and 2 was elevated to the power of said difference [$2^{(C_{tn} - C_{tmt})}$], and results were expressed as fold change relative to NZH cows.

Enzyme Activity

Citrate synthase (CS) activity was determined in 60 $\mu\text{g}/\text{mL}$ of liver homogenates based on the formation of 5-thio-2-nitrobenzoic acid at $\lambda = 412 \text{ nm}$ ($\epsilon_{412} = 13,700 \text{ L}/\text{mol}\cdot\text{cm}$) in the presence of 20 mM Tris-HCl pH 8, 300 μM acetyl-CoA, 500 μM oxaloacetate, and 100 μM 5,5'-dithio-bis (2-nitrobenzoic acid; García-Roche et al., 2019). Assays were performed in duplicate using a final volume of 200 μL in a Multiskan FC Microplate Photometer (Thermo Fisher Scientific).

Succinate dehydrogenase (SDH) activity was determined in 120 $\mu\text{g}/\text{mL}$ of mitochondrial protein based on the reduction of 2,6-dichlorophenolindophenol (DCPIP) by decylubiquinone at $\lambda = 600 \text{ nm}$ ($\epsilon_{600} = 21,000 \text{ L}/\text{mol}\cdot\text{cm}$) in the presence of 50 μM DCPIP, 1 mM potassium cyanide, 5 μM rotenone, and 50 μM decylubiquinone in a 25 mM phosphate buffer, pH 7.2. To quantify enzyme activity, baseline was subtracted from absorbance after addition of 10 mM succinate (Casal et al., 2018). Assays were performed in duplicate at 37°C using a final volume of 500 μL in a UV-2401 PC spectrophotometer (Shimadzu Corp.).

Western Blots

Liver homogenates were prepared with a lysis buffer complemented with protease and phosphatase inhibitors: 1 mM phenylmethylsulfonyl fluoride, supplemented with SigmaFAST protease inhibitor cocktail and Calbiochem phosphatase inhibitor cocktail (Sigma-Aldrich; García-Roche et al., 2019). Protein content was determined with a Bradford assay using BSA as standard (Bradford, 1976), and samples were kept at -80°C until analysis. Liver homogenates were resolved (30 μg) in 12% Tris-glycine SDS/PAGE, along with protein ladders (SDS7B2, Sigma-Aldrich), and proteins were transferred overnight to nitrocellulose membranes. Membranes were blocked with blocking buffer (Tris-buffered saline with 0.1% Tween 20 and 0.5% skim milk) and incubated overnight at 4°C with primary antibodies against GAPDH (1:1,000, Abcam, ab9485), succinate dehydrogenase subunit A (SDHA, 1:2000,

Abcam, ab14715), AMPK α (1:1,000, no. 2532, Cell Signaling Technology), and phosphoAMPK α (1:1,000, no. 2535, Cell Signaling Technology). For protein detection, membranes were washed and probed with secondary antibodies from LI-COR Biosciences: anti-mouse (1:10,000, IRDye 680, 926-68070) or anti-rabbit (1:20,000, IRDye 800, 926-32211). Immunoreactive proteins were detected with an infrared fluorescence detection system (Odyssey, LI-COR Biosciences), and bands were quantified with ImageStudio software (LI-COR Biosciences, version 2.0) by densitometry, and protein levels were normalized by protein levels of GAPDH the loading control.

Statistical Analysis

Data were analyzed in a randomized block design using SAS Academic Edition (SAS OnDemand for Academics, SAS Institute Inc.), with cow as the experimental unit. Univariate and linear regression analyses were performed for all variables to identify outliers and inconsistencies and to verify normality of residuals. Variance homogeneity was tested using the Levene, Bartlett, and Brown-Forsythe tests. When data did not have normal distribution or variance was not homogeneous, logarithmic transformations were performed to more closely approximate normality and homogeneity requirements. Values were removed when the studentized residual was >3 and <-3 ; no more than 3 values per variable were excluded. Least squares means and pooled standard error values of all variables are presented as non-transformed data to aid in comparison among variables.

Data were analyzed using the MIXED procedure; the model included Holstein strain as a fixed effect and year and block as random effects. Compound symmetry was used as the covariance structure, and the Kenward-Roger procedure was used to adjust the denominator degrees of freedom. Least squares means tests were conducted to analyze differences between groups. Means were considered to differ when $P < 0.05$, and a trend was declared when $0.05 < P < 0.10$. Pearson correlations were calculated with the CORR procedure.

RESULTS

Body Condition Score, Milk Yield, and Milk Composition

In average, for the 3 years evaluated, mid-lactation (at $174 \pm 23 \text{ d}$) milk yield was 20% higher for the NAH than the NZH strain ($P < 0.001$, Table 2). However, fat and protein percentages were 12 and 14% greater

Table 2. Milk yield and composition and BCS of mid-lactation New Zealand (NZH) and North American (NAH) cows in a pasture-based system, 3-yr average

Item	Strain ¹			<i>P</i> -value
	NZH	NAH	SEM ²	
Milk yield (kg/d)	24.0	30.0	1.0	<0.01
Fat (kg/d)	1.06	1.06	0.14	0.97
Fat (%)	4.58	4.01	0.15	<0.01
Protein (kg/d)	0.86	0.84	0.10	0.66
Protein (%)	3.70	3.17	0.04	<0.01
Lactose (kg/d)	1.10	1.24	0.14	<0.05
Lactose (%)	4.76	4.72	0.04	0.23
SCM ³ (kg/d)	25.7	26.4	1.2	0.39
Milk urea nitrogen (mg/dL)	24.3	21.6	0.6	<0.0001
BCS (units)	2.59	2.53	0.10	0.18

¹NZH = New Zealand Holstein (n = 12); NAH = North American Holstein (n = 18).

²All data shown as LSM ± SEM.

³SCM (kg) = solids-corrected milk; calculated as 12.3(F) + 6.56 (SNF) – 0.0752(M), where F, SNF, and M are expressed as kg of fat, solids-not-fat, and milk, respectively (Tyrrell and Reid, 1965).

for NZH than NAH cows ($P < 0.001$). This resulted in similar SCM yields between strains ($P = 0.39$). In line with the higher protein percentage for the NZH strain, milk urea nitrogen was approximately 11% greater for this strain ($P < 0.0001$). No differences were observed for BCS between strains either ($P = 0.18$).

Plasma and Hepatic Metabolites

Plasma glucose was 25% higher for the NZH versus the NAH strain ($P < 0.001$, Table 3), although no differences were found between cow strains in plasma urea ($P = 0.14$), NEFA ($P = 0.53$), or BHB ($P = 0.57$) concentrations. Neither concentrations of hepatic free glucose ($P = 0.17$), glycogen ($P = 0.18$), or triglyceride ($P = 0.68$) nor the ratios of free glucose to glycogen ($P = 0.94$) or triglyceride to glycogen ($P = 0.51$) in liver differed between Holstein strains.

Mitochondrial Function

Oxygen consumption rates were measured in liver biopsies after the addition of specific substrates for mitochondrial chain complexes I and II, and respiratory parameters were calculated (Table 4 and Figure 1A and 1B, respectively). Oligomycin-sensitive respiration was 1.3- to 1.4-fold greater for NZH than NAH cows ($P < 0.05$) when complex I and complex II substrates were used (Figure 1C and 1D, respectively). In addition, the maximum respiratory rate was calculated for both glutamate- and malate-driven (Figure 1E) and succinate-driven respiration (Figure 1F). For glutamate- and malate-driven respiration, the maximum respiratory

Table 3. Plasma and hepatic metabolites

Metabolite	Strain ¹			<i>P</i> -value
	NZH	NAH	SEM ²	
Plasma glucose (mmol/L)	3.54	2.81	0.17	0.0001
Plasma urea (mmol/L)	6.00	5.42	0.38	0.14
Plasma NEFA ³ (mmol/L)	0.124	0.116	0.02	0.53
Plasma BHB (mmol/L)	0.42	0.39	0.04	0.57
Liver triglyceride (mg/mg of liver protein)	2.65	2.67	0.45	0.68
Free liver glucose (mmol/g)	0.011	0.010	0.004	0.17
Hepatic glycogen (mg/mg of liver tissue)	2.21	1.92	0.17	0.18
Triglyceride/glycogen ratio ⁴	1.45	1.70	0.4	0.51
Free glucose/glycogen ratio	0.0049	0.0057	0.0021	0.94

¹NZH = New Zealand Holstein (n = 11–12); NAH = North American Holstein (n = 13–14).

²All data shown as LSM ± SEM.

³NEFA = nonesterified fatty acids.

⁴Liver triglyceride was corrected for milligrams of liver tissue, for appropriate comparison.

rate tended to be 1.2-fold higher for NZH than NAH cows ($P = 0.05$, Figure 1E); for succinate-driven respiration, the maximum respiratory rate was almost 2-fold greater for NZH versus NAH cows ($P < 0.001$, Figure 1F). Also, state 3 respiration and oligomycin-resistant respiration were higher ($P < 0.01$) in NZH than NAH cows only when succinate was used as substrate. The leaking control ratio—an index of proton leak—was higher for NAH than for NZH cows when complex I substrates were used ($P < 0.05$). However, it did not differ among strains when assessing complex II (0.61 vs. 0.66 ± 0.04 , NAH and NZH respectively, $P = 0.16$). Finally, non-mitochondrial respiration did not differ between strains.

Mitochondrial Mass

New Zealand Holstein cows presented greater hepatic mitochondrial abundance than NAH cows (Figure 2), measured as both mtDNA:nDNA ratio (1.04 vs. 0.69 ± 0.10 , $P < 0.05$, 2A) and CS activity (16.5 vs. 10.7 ± 1.9 mU/mg of protein, $P < 0.05$, Figure 2B) in liver homogenates.

Succinate Dehydrogenase Enzyme Activity and Protein Levels

Hepatic SDH activity did not differ between strains; however, when normalized by mitochondrial content assessed by CS activity, it tended ($P = 0.08$) to be 1.3-fold greater in the NAH strain (Table 5). Nevertheless, hepatic SDHA protein levels, assessed by western blot, did not differ between groups (Supplemental Figure S1, <https://data.mendeley.com/datasets/gx5yh5t2bp/1>).

Table 4. Complex I- and II-dependent respiratory parameters of NZH and NAH cows in a pasture-based system during mid-lactation, 3-yr average

Item	Strain ¹		SEM ²	P-value
	NZH	NAH		
Complex I respiratory parameters ³				
State 3 respiration	12.4	10.7	1.3	0.13
State 4 respiration	6.0	6.2	1.8	0.74
Maximum respiratory rate	14.3	11.5	1.9	0.05
Oligomycin-resistant respiration	6.7	6.3	1.1	0.42
Oligomycin-sensitive respiration	6.1	4.3	1.9	<0.05
Non-mitochondrial respiration	6.6	6.1	1.0	0.38
Leaking control ratio	0.53	0.62	0.04	<0.05
Complex II respiratory parameters ³				
State 3 respiration	35.7	21.3	5.8	0.001
State 4 respiration	22.7	16.3	2.9	<0.05
Maximum respiratory rate	50.2	26.7	9.0	<0.001
Oligomycin-resistant respiration	25.3	16.7	5.1	<0.01
Oligomycin-sensitive respiration	9.3	5.2	1.1	<0.05
Non-mitochondrial respiration	7.3	8.7	1.0	0.18
Leaking control ratio	0.61	0.66	0.04	0.16

¹NZH = New Zealand Holstein strain (n = 12); NAH = North American Holstein strain (n = 18).

²All data shown as LSM ± SEM.

³Oxygen consumption rate measurements of liver biopsies were obtained after addition of 10 mM glutamate and 5 mM malate or succinate, 4 μM ADP, 2 μM oligomycin, up to 4 μM carbonyl cyanide-p-trifluoromethoxyphenylhydrazone and 0.5 μM rotenone, and 2.5 μM antimycin. Oxygen consumption rates are expressed as pmol of O₂/min per mg of wet weight.

Gene Expression of Gluconeogenic Enzymes

Hepatic expression of *PC*, *PCK1*, and *PDK4* mRNA was at least 2-fold greater ($P < 0.01$) for NAH than for NZH cows (Figure 3), whereas *SDHA*, *G6PC*, *MMUT*, *PDHA1*, *PPARGC1A*, and *SIRT1* mRNA did not differ between groups (Table 6). In addition, the *PC:PCK1* ratio tended to be more elevated for NAH than NZH cows (2.00 vs. 1.41, $P = 0.08$). Milk yield and glycogen reserves were negative correlated ($r = -0.56$ and $P < 0.05$), whereas positive correlations were found between *PC* and *PCK1* mRNA ($r = 0.90$ and $P < 0.0001$) and *PC* and *PDK* mRNA ($r = 0.51$ and $P < 0.05$). Additionally, milk yield and *PC* mRNA and milk yield and *PCK1* mRNA were positively correlated ($r = 0.62$ and $P < 0.01$ for both).

The *PPARGC1A*, *SIRT1*, and *AMPK* Axis

No differences were found in hepatic gene expression of *PPARGC1A* (1.93 vs. 0.84 ± 0.31 relative mRNA abundance, NZH and NAH respectively, $P = 0.13$) or *SIRT1* (1.75 vs. 2.04 ± 0.26 relative mRNA abundance, NZH and NAH respectively, $P = 0.46$). Moreover, nei-

Table 5. Succinate dehydrogenase enzyme activity and protein levels in NZH and NAH cows in a pasture-based system during mid-lactation

Item ¹	Strain ²		SEM ³	P-value
	NZH	NAH		
SDH (mU/mg)	28.5	29.4	4.1	0.89
SDH:CS	1.65	2.54	0.3	0.08
SDHA (relative protein abundance)	1.07	1.01	0.09	0.69

¹SDH = succinate dehydrogenase; CS = citrate synthase; SDHA = succinate dehydrogenase subunit A.

²NZH = New Zealand Holstein (n = 11); NAH = North American Holstein (n = 11).

³All data shown as LSM ± SEM.

ther abundance of AMPK protein nor phosphorylated AMPK (pAMPK) protein differed between NAH and NZH cows (Table 7; Supplemental Figure S2, <https://data.mendeley.com/datasets/gx5yh5t2bp/1>).

DISCUSSION

Our findings indicated differences in hepatic energy metabolism between NZH and NAH cows in a pasture-based system during mid-lactation, observed in mitochondrial function, mitochondrial density, and mRNA expression of gluconeogenic genes. Production performance between NZH and NAH strains in pasture-based systems has been studied extensively; in fact, previous studies have found that although NAH cows produced more milk, the greater milk solids content of NZH cows accounted for no differences in milk solids yield between Holstein strains (Kolver et al., 2000; Lucy et al., 2009). Indeed, in the present study, during mid-lactation in a pasture-based system, with a supplementation of 33% of predicted intake, we found that despite milk yield being greater for NAH than NZH cows, fat and protein concentrations were greater for NZH than NAH, which resulted in similar SCM yields for both strains; this is consistent with previous studies (Kolver et al., 2000; White et al., 2012; Talmón et al., 2020). In line with greater protein concentration for NZH than NAH cows, milk urea nitrogen was also greater; however, plasma urea was not affected by strain and coincided with levels reported in other pasture-based systems (Bargo et al., 2002). Although a greater BCS for NZH than NAH cows could be expected (Kolver et al., 2002), Patton et al. (2009) reported, in agreement with our results, no differences between strains in BCS in a mid-lactation study. This could be a limitation of the present work, because a single moment of lactation and season is studied. Data from the larger study, where the herd

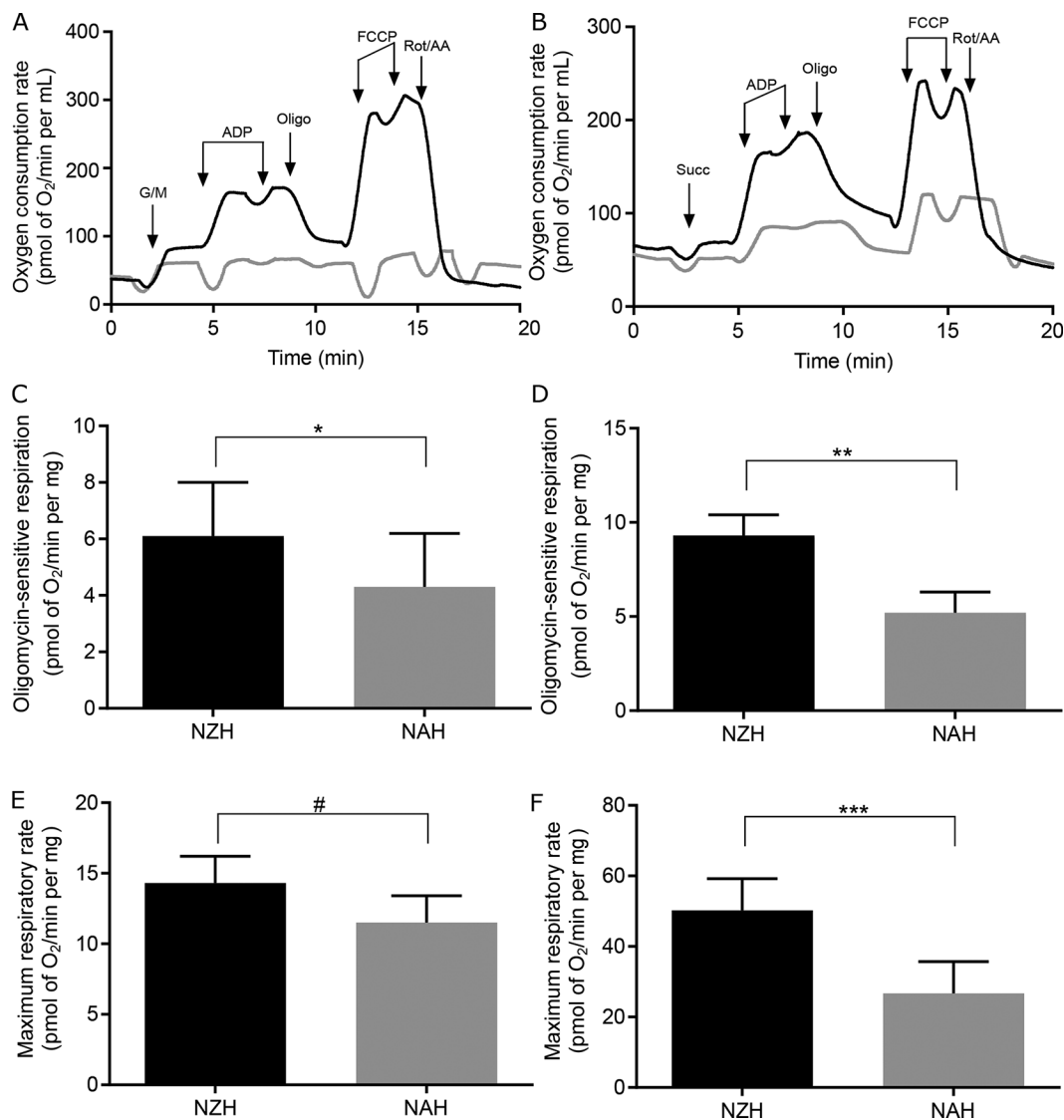


Figure 1. Mitochondrial function of New Zealand (NZH, $n = 12$) and North American (NAH, $n = 18$) cows in a pasture-based system during mid-lactation, 3-yr average. Oxygen consumption rates were measured in liver biopsies before and after the sequential addition of 10 mM glutamate and 5 mM malate (G/M; A, C, and E) or 20 mM succinate (Succ) (B, D, and F), 4 μ M ADP, 2 μ M oligomycin (Oligo), up to 4 μ M carbonyl cyanide-p-trifluoromethoxyphenylhydrazone (FCCP), and 0.5 μ M rotenone and 2.5 μ M antimycin (Rot/AA). Panels A and B show representative traces of oxygen consumption rates obtained for liver biopsies of NZH (black) and NAH (gray) cows. C and D show oligomycin-sensitive respiration, and E and F show maximum respiratory rate, obtained from oxygen consumption rate measurements performed as described in A and B. * $P < 0.05$, ** $P < 0.01$, *** $P < 0.001$, and # $0.05 < P < 0.10$. Data represent LSM \pm SEM.

is taken into consideration during 2 years, points out that mean BCS was lower for the NAH than for the NZH strain (Stirling et al., 2021).

Negative energy balance markers such as plasma NEFA, plasma BHB, and liver triglyceride did not indicate subclinical ketosis (>1.0 mmol/L of plasma BHB) or clinical fatty liver ($>10\%$ liver triglyceride wet weight; Bobe et al., 2004; Meikle et al., 2004) and were similar to previously reported values for mid- to late lactation in grazing conditions (García-Roche et al., 2021). However, the NZH cows had greater plasma

glucose concentrations than the NAH cows, probably due to greater glucose uptake by the mammary gland (Bell and Bauman, 1997), as milk yield in NAH cows was greater.

Liver energy homeostasis is crucial to maintain 2 major pathways in dairy cows: gluconeogenesis and detoxification of ammonia via the urea cycle (White, 2020). Oxidative phosphorylation provides the main source for ATP in the cell, and this is the predominant function of mitochondria. Additionally, mitochondria are dynamically regulated to cater for a broad spectrum of energy-

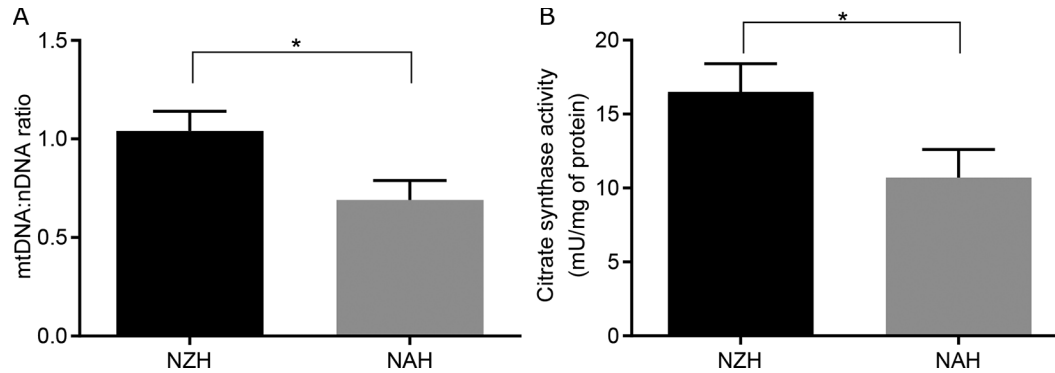


Figure 2. Mitochondrial abundance in New Zealand (NZH, $n = 11$) and North American (NAH, $n = 11$) cows in a pasture-based system during mid-lactation, 3-yr average. (A) Ratio of mitochondrial DNA to nuclear DNA (mtDNA:nDNA) assessed by real-time PCR in liver biopsies of NZH (black) and NAH (gray) cows. Results are expressed relative to NZH cows. (B) Citrate synthase activity measured in liver biopsies of NZH (black) and NAH (gray) cows. Data represent LSM \pm SEM. * $P < 0.05$.

demanding situations, and their inability to respond adequately may be considered an impairment (Brand and Nicholls, 2011). Our previous work found that, in grazing cows, mitochondrial function was impaired during early lactation, which was correlated with increased liver triglyceride content as well as protein acetylation, but restored toward late lactation (García-Roche et al., 2019). However, this study indicated differences in mitochondrial function between Holstein strains during mid-lactation in a pasture-based system. Parameters related to ATP synthesis and maximum respiratory rate were increased for NZH compared with NAH cows; differences were more dramatic when complex II substrates were used. In spite of this, when evaluating the isolated activity of SDH, which evaluates only the catalytic oxidoreductase activity, it tended to be increased for NAH compared with NZH cows, suggesting that decreased respiratory parameters when

complex II substrates were used in NAH cows may be related to overall oxidative phosphorylation capacity impairment (Bandara et al., 2021). Indeed, in human models, mitochondrial complex II is related to respiratory reserve capacity and is increased when PDK is inhibited (Pfleger et al., 2015); consistent with this, in our study hepatic *PDK4* was greater in NAH than NZH cows. Also, a recent study developed an SDH subunit D (SDHD) knockout mutant in human kidney cells and demonstrated that this decreased not only complex II-dependent respiration but also complex I-dependent respiration, given the repercussion of SDHD in the TCA cycle, which could have decreased the synthesis of reduction equivalents (Bandara et al., 2021).

Along with the assessment of parameters related to ATP synthesis, we also assessed proton leak—a phenomenon that consumes part of the protonmotive force and thus compromises ATP turnover—by means of the leaking control ratio (Brand and Nicholls, 2011; Koliaki et al., 2015) and found it was higher for NAH than for NZH cows ($P < 0.05$) when complex I substrates were used, although this was not the case when complex II substrates were used ($P = 0.16$). It is important to

Table 6. Hepatic expression of gluconeogenic enzyme genes for NZH and NAH cows in a pasture-based system during mid-lactation

Gene ¹	Strain ²		SEM ³	P-value
	NZH	NAH		
<i>SDHA</i>	1.45	1.69	0.21	0.28
<i>PC</i>	0.76	2.23	0.33	<0.01
<i>PCK1</i>	0.54	1.11	0.11	<0.01
<i>PDK4</i>	0.48	0.95	0.21	<0.05
<i>G6PC</i>	2.30	2.05	0.50	0.50
<i>MMUT</i>	0.43	0.50	0.11	0.37
<i>PDHA1</i>	2.02	1.82	0.29	0.62

¹Genes: glucose-6-phosphatase (*G6PC*), methylmalonyl-CoA mutase (*MMUT*), succinate dehydrogenase complex, subunit A, flavoprotein (Fp) (*SDHA*), pyruvate carboxylase (*PC*), phosphoenolpyruvate carboxykinase (*PCK1*), pyruvate dehydrogenase E1 subunit α 1 (*PDHA1*), pyruvate dehydrogenase kinase (*PDK4*).

²NZH = New Zealand Holstein ($n = 11$); NAH = North American Holstein ($n = 11$).

³All data shown as LSM \pm SEM.

Table 7. Protein abundance of AMPK and pAMPK for NZH and NAH cows in a pasture-based system during mid-lactation

Protein ¹	Strain ²		SEM ³	P-value
	NZH	NAH		
AMPK	1.00	1.11	0.095	0.47
pAMPK	1.06	1.16	0.177	0.61
pAMPK/AMPK	1.07	0.99	0.200	0.54

¹AMPK = AMP-activated protein kinase; pAMPK = phosphorylated AMP-activated protein kinase.

²NZH = New Zealand Holstein ($n = 11$); NAH = North American Holstein ($n = 11$).

³All data shown as LSM \pm SEM.

bear in mind that studies assessing mitochondrial function by respiration measure the respiration rate, which represents the proton current generated by substrate oxidation, which then flows through the protonmotive force and is afterward divided between proton leak and ATP turnover (Brand and Nicholls, 2011). Hence, differences between 2 groups of animals can be observed at different levels of ATP turnover and steady levels of proton leak, or vice-versa, or even at different levels of both ATP turnover and proton leak.

In general terms, functional loss of any of the complex II subunits could account for the lower complex II and complex I respiration in NAH cows. It has been widely reported that functional loss or inhibition of complex II could lead to reactive oxygen species, which could further damage mitochondrial function (Dröse, 2013; Hadrava Vanova et al., 2020). An impairment of

mitochondrial function can result in a deficient energy supply and hinder hepatic functions further progressing in disease, such as nonalcoholic fatty liver (Rector et al., 2010) and insulin resistance (Galgani et al., 2008; Peinado et al., 2014), as shown in mice and human models.

White et al. (2012) determined mRNA expression of gluconeogenic genes and hypothesized that NAH cows had decreased TCA cycling compared with NZH cows. Possible causes that explain impairment of the TCA cycle, a major contributor of reduction equivalents, are related to depletion of intermediates, yielding a drop in NADH/NAD⁺ ratios to the detriment of ATP synthesis (Burgess et al., 2004). Indeed, the TCA cycle in the dairy cow represents a major point of control, where oxaloacetate and acetyl-CoA are located in the crossroads; oxaloacetate levels may be depleted due

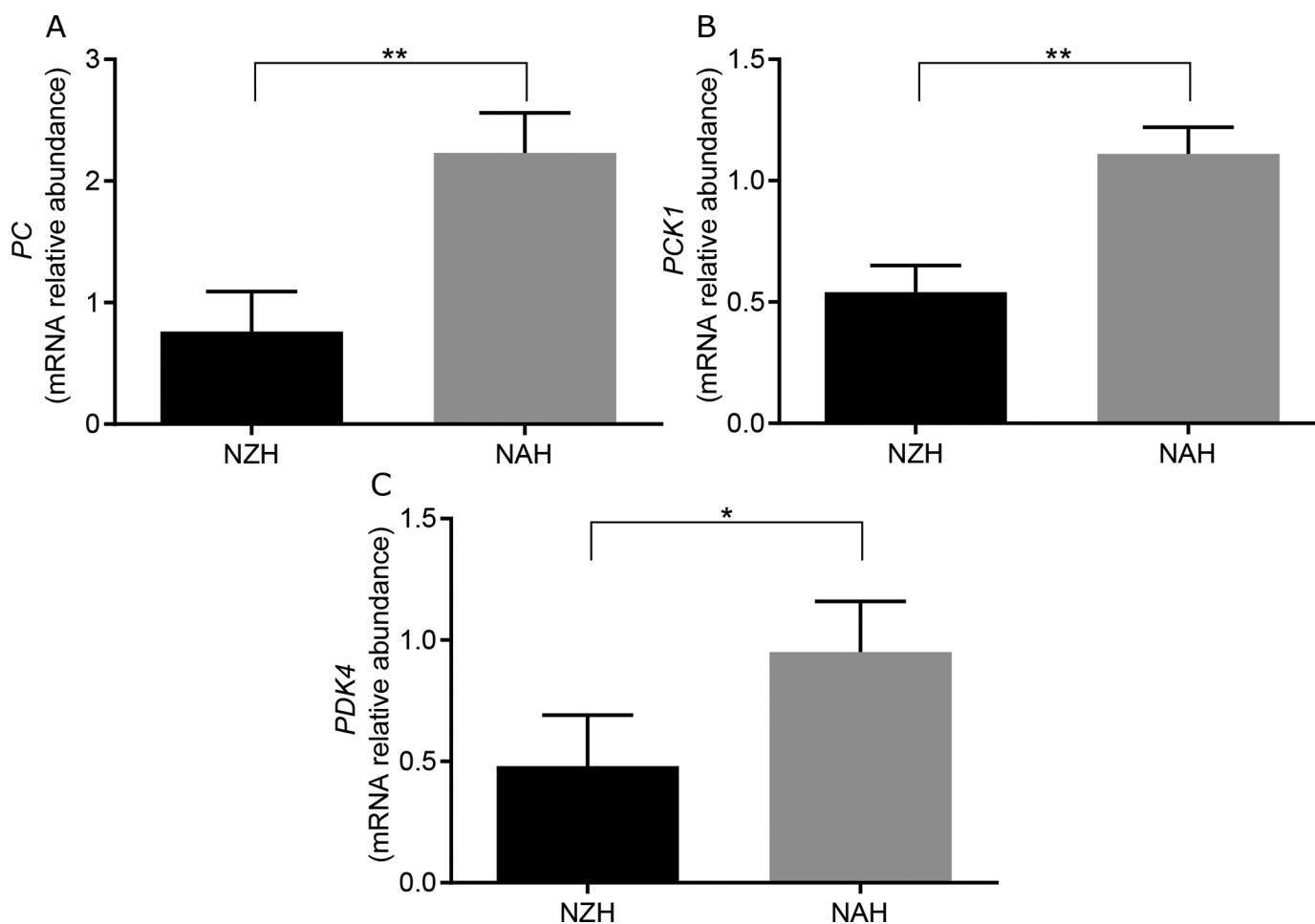


Figure 3. Hepatic gene expression of *PC*, *PCK1*, and *PDK4* for New Zealand Holstein (NZH) and North American Holstein (NAH) cows in a pasture-based system during mid-lactation. (A) Relative mRNA abundance of *PC* in liver biopsies of NZH (black, n = 11) and NAH (gray, n = 11) cows. (B) Relative mRNA abundance of *PCK1* in liver biopsies of NZH (black, n = 11) and NAH (gray, n = 11) cows. (C) Relative mRNA abundance of *PDK4* in liver biopsies of NZH (black, n = 11) and NAH (gray, n = 11) cows. * $P < 0.05$, and ** $P < 0.01$. Data represent LSM \pm SEM.

to demanding levels of gluconeogenesis (Allen, 2014; White, 2015), and acetyl-CoA concentration may be overloaded due to high levels of fatty acid oxidation, especially during early lactation (Adewuyi et al., 2005), or acetyl-CoA levels may be decreased as pyruvate is used for gluconeogenesis (Akbar et al., 2013).

In our work, NAH cows showed increased mRNA expression of key enzymes of gluconeogenesis (*PC*, *PCK1*, *PDK4*) compared with NZH cows. In addition, as lactation progresses, NZH cows reduced metabolizable energy intake and milk yield compared with NAH cows (Talmón et al., 2020). Indeed, the positive correlation between milk yield and *PCK1* mRNA, the rate-limiting step of gluconeogenesis, confirmed that gluconeogenesis is the driver of milk production (Aschenbach et al., 2010). In addition, the *PC:PCK1* ratio tended to be higher for NAH than NZH cows, indicating that oxaloacetate for gluconeogenesis was derived from precursors other than propionate (Weld et al., 2019). Moreover, *MMUT* mRNA levels in this work were similar to those previously reported in pasture-fed cows, lower than those of cows fed TMR (García-Roche et al., 2021). This emphasizes the relevance of turning to mobilization of lipid and protein reserves for alternative gluconeogenic precursors in a pasture-based system and was in agreement with the increased *PC* mRNA abundance in NAH versus NZH cows. In fact, the positive correlation between *PC* and *PCK1* mRNA suggests that gluconeogenesis is mostly sustained by gluconeogenic precursors that enter the pathway at the pyruvate carboxylase step. Similar positive correlations are observed between milk yield and *PC* mRNA and milk yield and *PCK1* mRNA. Furthermore, studies performed in dairy cows with propionate infusions have pointed out that mitochondrial increases of the NADH/NAD⁺ ratio may cause malate to be shunted toward gluconeogenesis, because mitochondrial malate dehydrogenase—the enzyme that catalyzes the conversion of malate to oxaloacetate—requires NAD⁺ (Zhang et al., 2015; Kennedy and Allen, 2019). This is especially relevant in models with propionate infusions, where the contribution of pyruvate from alternative precursors—evidenced by *PC* mRNA abundance—in the gluconeogenic pathway is scarce (Zhang et al., 2015). In our study, in contrast, we did find a relevant contribution of pyruvate from alternative precursors in the gluconeogenic pathway, as the correlations between *PC* and *PCK1* mRNA and *PC* mRNA and milk yield were positive. By contrast, succinate dehydrogenase, an enzyme that has a role in electron transfer in the respiratory chain and also catalyzes a step in the TCA cycle in between propionate conversion to methylmalonyl-CoA and oxaloacetate formation, showed greater activity for NAH than for NZH cows, when corrected by mitochondrial mass. Hence, it

is possible that gluconeogenesis from propionate and non-propionate precursors was increased in NAH cows. Neither abundance of mRNA and protein of SDHA nor abundance of *MMUT* mRNA differed between Holstein strains. Transcriptional or translational regulation of the steps that mediate mitochondrial propionate conversion into oxaloacetate to supply gluconeogenesis in bovine liver, which are little-known, could explain these results (Aschenbach et al., 2010).

In this work, we found that both *PCK1* mRNA and *PC* mRNA were increased in NAH cows; however, a previous work studying the expression of gluconeogenesis enzyme genes in different Holstein strains during early lactation while feeding less concentrate that the current study (White et al., 2012) found no differences in *PCK1* mRNA and that *PC* mRNA tended to be increased in NZH compared with NAH cows. These contrasting results could be due to differences in stage of lactation and level of supplementation, as both lactation stage and nutrition affect *PC* mRNA expression in dairy cattle (Greenfield et al., 2000; Velez and Donkin, 2005; García-Roche et al., 2021).

It is well established that glucose requirements of the gravid uterus increase appreciably during the latter half of pregnancy (Bell and Bauman, 1997). However, glucose demands of the gravid uterus might not have had a definitive effect in our results, because all the animals in this study were in the first trimester of pregnancy. Nonetheless, if the intrinsic differences in glucose metabolism observed among strains in this work during mid-lactation were also present during early lactation, this could in part explain the higher number of services per conception reported in the NAH versus the NZH strain in a maximum pasture treatment (Stirling et al., 2021), as low blood glucose concentrations after calving are associated with infertility in postpartum dairy cows (Green et al., 2012; Lucy et al., 2013).

Although we found no differences in hepatic *PDHA* expression, *PDK4* mRNA was greater for NAH than for NZH cows, further confirming that gluconeogenic precursors such as alanine and lactate would be channeled toward oxaloacetate instead of acetyl-CoA, as PDH activity is inhibited by PDK4 phosphorylation (Akbar et al., 2013). Studies in human and mice models have shown that downregulation of PDK4 increased ATP production, as it favors oxidative phosphorylation by yielding acetyl-CoA to the TCA cycle (Crewe et al., 2017; Liu et al., 2017). In line with our results, a previous study in mid-lactation feed-restricted cows found a downregulation of complex I proteins and upregulation of the gluconeogenic genes *PC* and *PDK4* (Akbar et al., 2013). Thus, impaired TCA cycling due to scarcity of the precursors oxaloacetate and acetyl-CoA could explain the reduced mitochondrial function related to

ATP synthesis in NAH cows relative to NZH cows. In sum, the hepatocyte of the lactating cow faces a rather controversial dilemma: gluconeogenesis versus energy production, sustained glucose output or healthy liver.

Mitochondrial function is crucial for cellular metabolism, and for this reason mitochondria have powerful feedback loops in order to maintain levels of ATP synthesis (Brand and Nicholls, 2011). One of the strategies used to face increasing energy demands is increase in mitochondrial density (Pesta et al., 2011). We studied mitochondrial abundance, measuring the maximum respiratory rate (García-Roche et al., 2018), CS activity, and mtDNA-to-nDNA ratio, and observed that they were increased for NZH compared with NAH cows. This could be a plausible mechanism to explain the ameliorated mitochondrial function in NZH cows. For instance, transition dairy cows with mild fatty liver have been found to present increased expression of oxidative phosphorylation complexes as well as mtDNA-to-nDNA ratio, probably as a response to impaired liver function due to lipid accumulation (Du et al., 2018). However, an increased ratio of mtDNA to nDNA, or any other proxy for mitochondrial abundance, does not necessarily reflect mitochondrial biogenesis and could also be a result of reduced degradation of damaged mitochondria, as observed previously in hepatic biopsies of human patients with nonalcoholic steatohepatitis (Koliaki et al., 2015). Increased mitochondrial abundance in cattle has been associated with increased adaptive capacity in several production systems. For instance, steers with low residual feed intake presented greater mitochondrial abundance and CS activity than steers with high residual feed intake; in other words, high-efficiency steers probably partitioned nutrients more efficiently toward energy metabolism (Casal et al., 2018). Moreover, a recent work carried out in high and low feed-efficient dairy cattle during weeks -4, 2, and 12 postpartum studied net fat oxidation, heat production, and mtDNA-to-nDNA ratio, and found that the high feed-efficient group had lower heat production (HP) per kilogram of metabolic BW ($BW^{0.75}$), as well as a higher number of relative mtDNA copies, pointing out that lower feed efficiency could result from fewer hepatic mitochondria and greater HP losses (Kennedy et al., 2021). Indeed, during yr 2 of the present study, our group studied energy partitioning and found that, at 192 DIM, residual HP per kilogram of $BW^{0.75}$ was lower in NZH than NAH cows. In particular, because HP is a function of maintenance and production, and no differences were found in retained energy among strains, differences in residual HP could be due to increased maintenance energy requirements of NAH cows (Talmón et al., 2020). Lower whole-body residual HP

and higher numbers of relative mtDNA copies, combined with increased mitochondrial function favoring ATP synthesis, suggests that NZH cows could indeed be more feed efficient than NAH cows (Kennedy et al., 2021).

We explored whether increases in mitochondrial mass and activity in NZH cows could be due to mitochondrial biogenesis. However, mRNA expression of *PPARGC1A* and *SIRT1*, which encode PGC1 α and SIRT1 master regulators of biogenesis (Cantó and Auwerx, 2009), did not differ between strains. Although gene expression was not altered in this study, protein expression and activity could be modulated by post-translational modifications, as protein expression of PGC1 α has been reported to be increased in dairy cows with increased mitochondrial abundance (Du et al., 2018). Indeed, a mechanism of PGC1 α activation is acetylation by SIRT1, and, in turn, SIRT1 is activated by AMPK by increasing levels of the oxidized electron carrier NAD⁺ (Cantó et al., 2009). Our recent work in dairy cattle in a TMR versus a pasture-based system showed that AMPK and its effector PGC1 α could be upregulating gluconeogenic genes, alongside its positive association with SIRT1 (García-Roche et al., 2021). However, we did not observe differential activation of this pathway between the 2 strains.

The activation of AMPK has been studied in cell culture and mice models and has been shown to modulate energy metabolism in response to high AMP or low ATP levels, and its effects include switching to catabolic pathways, enhancing oxidative phosphorylation, and, as a result, inducing complete oxidation (Cantó et al., 2009; Jenkins et al., 2013). The present results did not show differences in phosphorylated AMPK for NZH versus NAH cows under pasture-based conditions during late mid-lactation. This could be explained, as previous authors have hypothesized, because the AMPK pathway is not an eligible indicator for whole-animal energy balance, as differences among cow groups with high and low liver fat contents were not elicited; however, its increase during early lactation is relevant (Schäff et al., 2012). To confirm this, we have previously shown that AMPK activation is a phenomenon that indeed takes place during early lactation but not during late lactation (García-Roche et al., 2021). Although it is possible that the AMPK signaling pathway does not play a significant role in cows of diverging strains during mid-lactation, the molecular mechanisms regulating hepatic nutrient partitioning still lack resolution of understanding. Hence, further studies emphasizing the activation of PGC1 α by means of post-translation modifications, its activity, and its effect on hepatic cellular energy metabolism of dairy cows, would be useful.

CONCLUSIONS

Our results showed that Holstein cows of New Zealand origin presented improved hepatic mitochondrial function compared with cows of North American origin during mid-lactation in a pasture-based system, as respiration parameters related to ATP synthesis were increased, while maintaining similar milk solids production. Furthermore, Holstein cows of North American origin have greater expression of gluconeogenic genes, which probably translates into decreased availability of reducing equivalents for oxidative phosphorylation, as neither pyruvate nor oxaloacetate are fueling the TCA cycle. In addition to improved mitochondrial function, Holstein cows of New Zealand origin had increased mitochondrial mass, which could be a plausible mechanism for augmenting the respiratory capacity. Although this work shows dramatic differences in hepatic cellular energy metabolism, further research is needed to elucidate the mechanistic regulation underlying this phenomenon. Moreover, information regarding cellular energy metabolism presented in this study could be useful for the selection of a genetic strain that is better adapted for a production system with a high inclusion of pastures.

ACKNOWLEDGMENTS

The authors thank all the staff of the Dairy Unit of the Experimental Station “La Estanzuela” (Semillero, Uruguay) for their support in animal handling, as well as Ezequiel Jorge-Smeding (Departamento de Producción Animal y Pasturas, Facultad de Agronomía, Universidad de la República, Montevideo, Uruguay) and Irene Benoit (Centro de Investigaciones Biomédicas and Departamento de Bioquímica, Facultad de Medicina, Universidad de la República, Montevideo) for support in the analysis of blood metabolites. MGR conceived and designed laboratory experiments, performed field and laboratory experiments, analyzed the results, and wrote the original draft and revised versions of the manuscript. MC conceptualized and designed field experiment, conceived and designed laboratory experiments, supervised field and laboratory experiments and results analyses, obtained funding and administrated the project, and reviewed and edited the manuscript. CQ conceived, designed, and supervised laboratory experiments, and reviewed and edited the manuscript. AC conceived, designed, and supervised laboratory experiments. AM conceptualized and designed the field experiment and obtained funding. DT, ALA, and GC performed field and laboratory experiments. All authors reviewed the manuscript and approved the final version of the manuscript. M. García-Roche was sup-

ported by Comisión Académica de Posgrados (Montevideo, Uruguay) fellowship BDDX_2018_1#49004502. D. Talmón was supported by Agencia Nacional de Investigación e Innovación (ANII) fellowship POS_NAC_2017_1_141266. A. Cassina and C. Quijano were partially funded by grants of the Espacio Interdisciplinario-Centros, Universidad de la República (UdelaR; Montevideo, Uruguay) 2015. A. Cassina was also supported by the grant Comisión Sectorial de Investigación Científica (CSIC) grupos I+D 2014 (767). The project was funded by CSIC of the UdelaR CSIC I+D 2018 ID 103 to M. Carriquiry and C. Quijano, as well as by ANII INNOVAGRO 2018: FSA_1_2018_1_152220 to M. Carriquiry and A. Cassina. A. Mendoza received funding from the project PL_21_0_00 of the Instituto Nacional de Investigación Agropecuaria (Semillero, Uruguay). The authors have not stated any conflicts of interest.

REFERENCES

- Adewuyi, A. A., E. Gruys, and F. J. C. M. Van Eerdenburg. 2005. Non esterified fatty acids (NEFA) in dairy cattle. A review. *Vet. Q.* 27:117–126. <https://doi.org/10.1080/01652176.2005.9695192>.
- Akbar, H., M. Bionaz, D. B. Carlson, S. L. Rodriguez-Zas, R. E. Everts, H. A. Lewin, J. K. Drackley, and J. J. Looor. 2013. Feed restriction, but not L-carnitine infusion, alters the liver transcriptome by inhibiting sterol synthesis and mitochondrial oxidative phosphorylation and increasing gluconeogenesis in mid-lactation dairy cows. *J. Dairy Sci.* 96:2201–2213. <https://doi.org/10.3168/jds.2012-6036>.
- Allen, M. S. 2014. Drives and limits to feed intake in ruminants. *Anim. Prod. Sci.* 54:1513–1524. <https://doi.org/10.1071/AN14478>.
- Armour, S. M., J. R. Remsburg, M. Damle, S. Sidoli, W. Y. Ho, Z. Li, B. A. Garcia, and M. A. Lazar. 2017. An HDAC3-PROX1 corepressor module acts on HNF4 α to control hepatic triglycerides. *Nat. Commun.* 8:549. <https://doi.org/10.1038/s41467-017-00772-5>.
- Aschenbach, J. R., N. B. Kristensen, S. S. Donkin, H. M. Hammon, and G. B. Penner. 2010. Gluconeogenesis in dairy cows: The secret of making sweet milk from sour dough. *IUBMB Life* 62:869–877. <https://doi.org/10.1002/iub.400>.
- Astessiano, A. L., A. Meikle, M. Fajardo, J. Gil, D. A. Mattiada, P. Chilibroste, and M. Carriquiry. 2015. Metabolic and endocrine profiles and hepatic gene expression of Holstein cows fed total mixed ration or pasture with different grazing strategies during early lactation. *Acta Vet. Scand.* 57:70. <https://doi.org/10.1186/s13028-015-0163-6>.
- Bancroft, G., and E. G. Fry. 1933. Adsorption and hydrolysis of glycogen. *J. Biol. Chem.* 100:255–265. [https://doi.org/10.1016/S0021-9258\(18\)76001-8](https://doi.org/10.1016/S0021-9258(18)76001-8).
- Bandara, A. B., J. C. Drake, and D. A. Brown. 2021. Complex II subunit SDHD is critical for cell growth and metabolism, which can be partially restored with a synthetic ubiquinone analog. *BMC Mol. Cell Biol.* 22:35. <https://doi.org/10.1186/s12860-021-00370-w>.
- Bargo, F., L. D. Muller, J. E. Delahoy, and T. W. Cassidy. 2002. Performance of high producing dairy cows with three different feeding systems combining pasture and total mixed rations. *J. Dairy Sci.* 85:2948–2963. [https://doi.org/10.3168/jds.S0022-0302\(02\)74381-6](https://doi.org/10.3168/jds.S0022-0302(02)74381-6).
- Bell, A. W., and D. E. Bauman. 1997. Adaptations of glucose metabolism during pregnancy and lactation. *J. Mammary Gland Biol. Neoplasia* 2:265–278. <https://doi.org/10.1023/A:1026336505343>.
- Bobbe, G., J. W. Young, and D. C. Beitz. 2004. Invited Review: Pathology, etiology, prevention, and treatment of fatty liver in dairy

- cows. *J. Dairy Sci.* 87:3105–3124. [https://doi.org/10.3168/jds.S0022-0302\(04\)73446-3](https://doi.org/10.3168/jds.S0022-0302(04)73446-3).
- Bradford, M. M. 1976. A rapid and sensitive method for the quantitation of microgram quantities of protein utilizing the principle of protein-dye binding. *Anal. Biochem.* 72:248–254. [https://doi.org/10.1016/0003-2697\(76\)90527-3](https://doi.org/10.1016/0003-2697(76)90527-3).
- Brand, M. D., and D. G. Nicholls. 2011. Assessing mitochondrial dysfunction in cells. *Biochem. J.* 437:575. <https://doi.org/10.1042/BJ4370575u>.
- Burgess, S. C., N. Hausler, M. Merritt, F. M. H. Jeffrey, C. Storey, A. Milde, S. Koshy, J. Lindner, M. A. Magnuson, C. R. Malloy, and A. D. Sherry. 2004. Impaired tricarboxylic acid cycle activity in mouse livers lacking cytosolic phosphoenolpyruvate carboxylase. *J. Biol. Chem.* 279:48941–48949. <https://doi.org/10.1074/jbc.M407120200>.
- Cantó, C., and J. Auwerx. 2009. PGC-1 α , SIRT1 and AMPK, an energy sensing network that controls energy expenditure. *Curr. Opin. Lipidol.* 20:98–105. <https://doi.org/10.1097/MOL.0b013e328328d0a4>.
- Cantó, C., Z. Gerhart-hines, J. N. Feige, M. Lagouge, L. Noriega, J. C. Milne, P. J. Elliott, P. Puigserver, and J. Auwerx. 2009. AMPK regulates energy expenditure by modulating NAD⁺ metabolism and SIRT1 activity. *Nature* 458:1056–1060. <https://doi.org/10.1038/nature07813>.
- Carriquiry, M., W. J. Weber, S. C. Fahrenkrug, and B. A. Crooker. 2009. Hepatic gene expression in multiparous Holstein cows treated with bovine somatotropin and fed n-3 fatty acids in early lactation. *J. Dairy Sci.* 92:4889–4900. <https://doi.org/10.3168/jds.2008-1676>.
- Casal, A., M. Garcia-Roche, E. A. Navajas, A. Cassina, and M. Carriquiry. 2018. Hepatic mitochondrial function in Hereford steers with divergent residual feed intake phenotypes. *J. Anim. Sci.* 96:4431–4443. <https://doi.org/10.1093/jas/sky285>.
- Chagas, L. M., F. M. Rhodes, D. Blache, P. J. S. Gore, K. A. Macdonald, and G. A. Verkerk. 2006. Precalving effects on metabolic responses and postpartum anestrus in grazing primiparous dairy cows. *J. Dairy Sci.* 89:1981–1989. [https://doi.org/10.3168/jds.S0022-0302\(06\)72265-2](https://doi.org/10.3168/jds.S0022-0302(06)72265-2).
- Chilibroste, P., D. A. Mattiauda, O. Bentancur, P. Soca, and A. Meikle. 2012. Effect of herbage allowance on grazing behavior and productive performance of early lactation primiparous Holstein cows. *Anim. Feed Sci. Technol.* 173:201–209. <https://doi.org/10.1016/j.anifeeds.2012.02.001>.
- Crewe, C., C. Schafer, I. Lee, M. Kinter, and L. I. Szewda. 2017. Regulation of pyruvate dehydrogenase kinase 4 in the heart through degradation by the Lon protease in response to mitochondrial substrate availability. *J. Biol. Chem.* 292:305–312. <https://doi.org/10.1074/jbc.M116.754127>.
- Dröse, S. 2013. Differential effects of complex II on mitochondrial ROS production and their relation to cardioprotective pre- and postconditioning. *Biochim. Biophys. Acta* 1827:578–587. <https://doi.org/10.1016/j.bbabi.2013.01.004>.
- Du, X., T. Shen, H. Wang, X. Qin, D. Xing, Q. Ye, Z. Shi, Z. Fang, Y. Zhu, Y. Yang, Z. Peng, C. Zhao, B. Lv, X. Li, G. Liu, and X. Li. 2018. Adaptations of hepatic lipid metabolism and mitochondria in dairy cows with mild fatty liver. *J. Dairy Sci.* 101:9544–9558. <https://doi.org/10.3168/jds.2018-14546>.
- Edmonson, A. J., I. K. Lean, L. D. Weaver, T. Farver, and G. Webster. 1989. A body condition scoring chart for Holstein dairy cows. *J. Dairy Sci.* 72:68–78.
- Fariña, S. R., and P. Chilibroste. 2019. Opportunities and challenges for the growth of milk production from pasture: The case of farm systems in Uruguay. *Agric. Syst.* 176:102631. <https://doi.org/10.1016/j.agsy.2019.05.001>.
- Galgani, J. E., C. Moro, and E. Ravussin. 2008. Metabolic flexibility and insulin resistance. *Am. J. Physiol. Endocrinol. Metab.* 295:E1009–E1017. <https://doi.org/10.1152/ajpendo.90558.2008>.
- García-Roche, M., G. Cañibe, A. Casal, D. A. Mattiauda, M. Ceriani, A. Jasinsky, A. Cassina, C. Quijano, and M. Carriquiry. 2021. Glucose and fatty acid metabolism of dairy cows in a total mixed ration or pasture-based system during lactation. *Front. Anim. Sci.* 2:622500. <https://doi.org/10.3389/fanim.2021.622500>.
- García-Roche, M., A. Casal, M. Carriquiry, R. Radi, C. Quijano, and A. Cassina. 2018. Respiratory analysis of coupled mitochondria in cryopreserved liver biopsies. *Redox Biol.* 17:207–212. <https://doi.org/10.1016/j.redox.2018.03.008>.
- García-Roche, M., A. Casal, D. A. Mattiauda, M. Ceriani, A. Jasinsky, M. Mastrogiovanni, A. Trostchansky, M. Carriquiry, A. Cassina, and C. Quijano. 2019. Impaired hepatic mitochondrial function during early lactation in dairy cows: Association with protein lysine acetylation. *PLoS One* 14:e0213780. <https://doi.org/10.1371/journal.pone.0213780>.
- Gnaiger, E. 2009. Capacity of oxidative phosphorylation in human skeletal muscle: New perspectives of mitochondrial physiology. *Int. J. Biochem. Cell Biol.* 41:1837–1845. <https://doi.org/10.1016/j.biocel.2009.03.013>.
- Green, J. C., J. P. Meyer, A. M. Williams, E. M. Newsom, D. H. Keisler, and M. C. Lucy. 2012. Pregnancy development from day 28 to 42 of gestation in postpartum Holstein cows that were either milked (lactating) or not milked (not lactating) after calving. *Reproduction* 143:699–711. <https://doi.org/10.1530/REP-11-0461>.
- Greenfield, R. B., M. J. Cecava, and S. S. Donkin. 2000. Changes in mRNA expression for gluconeogenic enzymes in liver of dairy cattle during the transition to lactation. *J. Dairy Sci.* 83:1228–1236. [https://doi.org/10.3168/jds.S0022-0302\(00\)74989-7](https://doi.org/10.3168/jds.S0022-0302(00)74989-7).
- Hadrava Vanova, K., M. Kraus, J. Neuzil, and J. Rohlena. 2020. Mitochondrial complex II and reactive oxygen species in disease and therapy. *Redox Rep.* 25:26–32. <https://doi.org/10.1080/13510002.2020.1752002>.
- Harris, B. L., and E. S. Kolver. 2001. Review of Holsteinization on intensive pastoral dairy farming in New Zealand. *J. Dairy Sci.* 84:E56–E61. [https://doi.org/10.3168/jds.S0022-0302\(01\)70197-X](https://doi.org/10.3168/jds.S0022-0302(01)70197-X).
- Jasinsky, A., D. A. Mattiauda, M. Ceriani, A. Casal, and M. Carriquiry. 2019. Heat production and body composition of primiparous Holstein cows with or without grazing pastures in early lactation. *Livest. Sci.* 225:1–7. <https://doi.org/10.1016/j.livsci.2019.04.017>.
- Jenkins, Y., T. Sun, V. Markovtsov, M. Foretz, W. Li, H. Nguyen, Y. Li, A. Pan, G. Uy, L. Gross, K. Baltgalvis, S. L. Yung, T. Gururaja, T. Kinoshita, A. Owyang, I. J. Smith, K. McCaughey, K. White, G. Godinez, R. Alcantara, C. Choy, H. Ren, R. Basile, D. J. Sweeny, X. Xu, S. D. Issakani, D. C. Carroll, D. A. Goff, S. J. Shaw, R. Singh, L. G. Boros, M.-A. Laplante, B. Marcotte, R. Kohen, B. Viollet, A. Marette, D. G. Payan, T. M. Kinsella, and Y. Hitoshi. 2013. AMPK activation through mitochondrial regulation results in increased substrate oxidation and improved metabolic parameters in models of diabetes. *PLoS One* 8:e81870. <https://doi.org/10.1371/journal.pone.0081870>.
- Kennedy, K. M., and M. S. Allen. 2019. Hepatic metabolism of propionate relative to meals for cows in the postpartum period. *J. Dairy Sci.* 102:7997–8010.
- Kennedy, K. M., F. Becker, H. M. Hammon, and B. Kuhla. 2021. Differences in net fat oxidation, heat production, and liver mitochondrial DNA copy numbers between high and low feed-efficient dairy cows. *J. Dairy Sci.* 104:9287–9303. <https://doi.org/10.3168/jds.2020-20031>.
- Koliaki, C., J. Szendroedi, K. Kaul, T. Jelenik, P. Nowotny, F. Jankowiak, C. Herder, M. Carstensen, M. Krausch, W. T. Knoefel, M. Schlensak, and M. Roden. 2015. Adaptation of hepatic mitochondrial function in humans with non-alcoholic fatty liver is lost in steatohepatitis. *Cell Metab.* 21:739–746. <https://doi.org/10.1016/j.cmet.2015.04.004>.
- Kolver, E. S., A. R. Napper, P. J. Copeman, and L. D. Muller. 2000. A comparison of New Zealand and overseas Holstein Friesian heifers. Pages 265–269 in *Proc. New Zealand Society of Animal Production*, Hamilton, New Zealand, vol. 60.
- Kolver, E. S., J. R. Roche, M. J. De Veth, P. L. Thorne, and A. R. Napper. 2002. Total mixed rations versus pasture diets: Evidence for a genotype \times diet interaction in dairy cow performance. Pages 246–251 in *Proc. New Zealand Society of Animal Production*, Palmerston North, New Zealand, vol. 62.

- Liu, X., R. Zuo, Y. Bao, X. Qu, K. Sun, and H. Ying. 2017. Down-regulation of PDK4 is critical for the switch of carbohydrate catabolism during syncytialization of human placental trophoblasts. *Sci. Rep.* 7:8474. <https://doi.org/10.1038/s41598-017-09163-8>.
- Lucy, M. C., R. C. Escalante, D. H. Keisler, W. R. Lamberson, and D. J. Mathew. 2013. Short communication: Glucose infusion into early postpartum cows defines an upper physiological set point for blood glucose and causes rapid and reversible changes in blood hormones and metabolites. *J. Dairy Sci.* 96:5762–5768. <https://doi.org/10.3168/jds.2013-6794>.
- Lucy, M. C., G. A. Verkerk, B. E. Whyte, K. A. Macdonald, L. Burton, R. T. Cursons, J. R. Roche, and C. W. Holmes. 2009. Somatotropic axis components and nutrient partitioning in genetically diverse dairy cows managed under different feed allowances in a pasture system. *J. Dairy Sci.* 92:526–539. <https://doi.org/10.3168/jds.2008-1421>.
- Meikle, A., M. de L. Adrien, D. A. Mattiauda, and P. Chilibroste. 2013. Effect of sward condition on metabolic endocrinology during the early postpartum period in primiparous grazing dairy cows and its association with productive and reproductive performance. *Anim. Feed Sci. Technol.* 186:139–147. <https://doi.org/10.1016/j.anifeedsci.2013.10.003>.
- Meikle, A., M. Kulcsar, Y. Chilliard, H. Febel, C. Delavaud, D. Cavestany, and P. Chilibroste. 2004. Effects of parity and body condition at parturition on endocrine and reproductive parameters of the cow. *Reproduction* 127:727–737. <https://doi.org/10.1530/rep.1.00080>.
- NRC. 2001. *Nutrient Requirements of Dairy Cattle*, 7th rev. ed. National Academies Press. <https://doi.org/10.17226/9825>.
- O'Callaghan, T. F., D. Hennessy, S. McAuliffe, K. N. Kilcawley, M. O'Donovan, P. Dillon, R. P. Ross, and C. Stanton. 2016. Effect of pasture versus indoor feeding systems on raw milk composition and quality over an entire lactation. *J. Dairy Sci.* 99:9424–9440. <https://doi.org/10.3168/jds.2016-10985>.
- Patton, J., J. J. Murphy, F. P. Omara, and S. T. Butler. 2009. Responses of North American and New Zealand strains of Holstein-Friesian dairy cattle to homeostatic challenges during early and mid-lactation. *Animal* 3:251–260. <https://doi.org/10.1017/S175173110800342X>.
- Peinado, J. R., A. Diaz-Ruiz, G. Fruhbeck, and M. M. Malagon. 2014. Mitochondria in metabolic disease: Getting clues from proteomic studies. *Proteomics* 14:452–466. <https://doi.org/10.1002/pmic.201300376>.
- Pesta, D., F. Hoppel, C. Macek, H. Messner, M. Faulhaber, C. Kobel, W. Parson, M. Burtscher, M. Schocke, and E. Gnaiger. 2011. Similar qualitative and quantitative changes of mitochondrial respiration following strength and endurance training in normoxia and hypoxia in sedentary humans. *Am. J. Physiol. Regul. Integr. Comp. Physiol.* 301:R1078–R1087. <https://doi.org/10.1152/ajpregu.00285.2011>.
- Pfaffl, M. W. 2004. Chapter 3: Quantification strategies in real-time polymerase chain reaction. Pages 89–113 in *A–Z of Quantitative PCR*. S. A. Bustin, ed. International University Line.
- Pfleger, J., M. He, and M. Abdellatif. 2015. Mitochondrial complex II is a source of the reserve respiratory capacity that is regulated by metabolic sensors and promotes cell survival. *Cell Death Dis.* 6:e1835. <https://doi.org/10.1038/cddis.2015.202>.
- Rector, R. S., J. P. Thyfault, G. M. Uptergrove, E. M. Morris, P. Naples, S. J. Borengasser, C. R. Mikus, M. J. Laye, M. H. Laughlin, F. W. Booth, and J. A. Ibdah. 2010. Mitochondrial dysfunction precedes insulin resistance and hepatic steatosis and contributes to the natural history of non-alcoholic fatty liver disease in an obese rodent model. *J. Hepatol.* 52:727–736. <https://doi.org/10.1016/j.jhep.2009.11.030>.
- Schäff, C., S. Borner, S. Hacke, U. Kautzsch, D. Albrecht, H. M. Hammon, M. Röntgen, and B. Kuhla. 2012. Increased anaplerosis, TCA cycling, and oxidative phosphorylation in the liver of dairy cows with intensive body fat mobilization during early lactation. *J. Proteome Res.* 11:5503–5514. <https://doi.org/10.1021/pr300732n>.
- Stirling, S., L. Delaby, A. Mendoza, and S. Fariña. 2021. Intensification strategies for temperate hot-summer grazing dairy systems in South America: Effects of feeding strategy and cow genotype. *J. Dairy Sci.* 104:12647–12663. <https://doi.org/10.3168/jds.2021-20507>.
- Talmón, D., M. Garcia-Roche, A. Mendoza, D. A. Mattiauda, and M. Carriquiry. 2020. Energy partitioning and energy efficiency of two Holstein genotypes under a mixed pasture-based system during mid and late lactation. *Livest. Sci.* 239:104166. <https://doi.org/10.1016/j.livsci.2020.104166>.
- Tyrrell, H. F., and J. T. Reid. 1965. Prediction of the energy value of cow's milk. *J. Dairy Sci.* 48:1215–1223. [https://doi.org/10.3168/jds.S0022-0302\(65\)88430-2](https://doi.org/10.3168/jds.S0022-0302(65)88430-2).
- Velez, J. C., and S. S. Donkin. 2005. Feed restriction induces pyruvate carboxylase but not phosphoenolpyruvate carboxylase in dairy cows. *J. Dairy Sci.* 88:2938–2948. [https://doi.org/10.3168/jds.S0022-0302\(05\)72974-X](https://doi.org/10.3168/jds.S0022-0302(05)72974-X).
- Weld, K. A., S. J. Erb, and H. M. White. 2019. Short communication: Effect of manipulating fatty acid profile on gluconeogenic gene expression in bovine primary hepatocytes. *J. Dairy Sci.* 102:7576–7582. <https://doi.org/10.3168/jds.2018-16150>.
- White, H. M. 2015. The role of TCA cycle anaplerosis in ketosis and fatty liver in periparturient dairy cows. *Animals (Basel)* 5:793–802. <https://doi.org/10.3390/ani5030384>.
- White, H. M. 2020. ADSA Foundation Scholar Award: Influencing hepatic metabolism: Can nutrient partitioning be modulated to optimize metabolic health in the transition dairy cow? *J. Dairy Sci.* 103:6741–6750. <https://doi.org/10.3168/jds.2019-18119>.
- White, H. M., S. S. Donkin, M. C. Lucy, T. M. Grala, and J. R. Roche. 2012. Short communication: Genetic differences between New Zealand and North American dairy cows alter milk production and gluconeogenic enzyme expression1. *J. Dairy Sci.* 95:455–459. <https://doi.org/10.3168/jds.2011-4598>.
- Zhang, Q., S. L. Koser, B. J. Bequette, and S. S. Donkin. 2015. Effect of propionate on mRNA expression of key genes for gluconeogenesis in liver of dairy cattle. *J. Dairy Sci.* 98:8698–8709. <https://doi.org/10.3168/jds.2015-9590>.

ORCID

- Mercedes García-Roche  <https://orcid.org/0000-0002-2759-8829>
- Daniel Talmón  <https://orcid.org/0000-0003-2284-4354>
- Guillermo Cañibe  <https://orcid.org/0000-0003-4485-2662>
- Alejandro Mendoza  <https://orcid.org/0000-0002-8517-6181>
- Celia Quijano  <https://orcid.org/0000-0001-9254-7123>
- Mariana Carriquiry  <https://orcid.org/0000-0002-1600-2591>